Flat resonances in one-dimensional quantum scattering

1996 J. Phys. A: Math. Gen. 29 7259

(http://iopscience.iop.org/0305-4470/29/22/021)

J. Phys. A: Math. Gen. **29** (1996) 7259–7277. Printed in the UK

Flat resonances in one-dimensional quantum scattering

L V Chebotarev† and A Tchebotareva‡

† Case Postale 655, Montreal, Quebec, Canada H2A 3N2

‡ Department of Physics, University of Montreal, Montreal, Quebec, Canada H3C 3J7

Received 18 June 1996, in final form 4 September 1996

In memory of Professor E A Kaner

Abstract. The existence of 'flat' resonances in one-dimensional quantum scattering is established. A 'flat' resonance is the vanishing of a particle's reflection coefficient $R(k)$, for some specific value $k = k_n$ of its wavenumber k, as the fourth power of the difference $\Delta k = k - k_n$, i.e. $R(k) \sim (\Delta k)^4$. Stokes' phenomenon in quantum scattering is found. It manifests itself as a drastic change in the reflection coefficient $R(k)$ as k passes through a certain critical value $k = k_c$ associated with the scattering potential $U(x)$. The first numerical verification of the semiclassical theory of resonances in one-dimensional scattering is obtained for very non-trivial potentials.

1. Introduction

Resonances in one-dimensional quantum scattering represent one of the most interesting, most important, and, at the same time, one of the least-studied effects among the fundamental quantum phenomena. In the physics of 1d conductors, the significance of resonances in 1d elastic scattering is evident in view of their impact on the mean free-flight time of electrons. Indeed, consider N_{imp} identical single impurities which are randomly positioned along a linear chain of length L on the x-axis. If the distribution of impurities is uniform, then the probability (referred to unit length) to find an impurity is $n_{\text{imp}} = N_{\text{imp}}/L$. Suppose that each impurity is described by a short-range potential $U(x)$ with a radius a of atomic scale. The distribution of impurities is supposed to be sparse, i.e. $n_{\text{imp}}a \ll 1$. The exact reflection amplitude r_k, relative to the scattering of an electron with the wavenumber k by an isolated impurity, is then obtained by solving the Schrödinger equation

$$-\frac{\hbar^2}{2m}\frac{\mathrm{d}^2\psi}{\mathrm{d}x^2} + U(x)\psi(x) = E\psi(x) \qquad (E > 0;\ E > U(x),\ -\infty < x < +\infty) \tag{1.1}$$

with standard boundary conditions

$$\begin{aligned} &\psi(x) \sim t_k \mathrm{e}^{\mathrm{i}kx} \qquad (x \to +\infty) \\ &\psi(x) \sim \mathrm{e}^{\mathrm{i}kx} + r_k \mathrm{e}^{-\mathrm{i}kx} \qquad (x \to -\infty) \end{aligned} \tag{1.2}$$

where t_k is the transmission amplitude for the wavenumber $k = \sqrt{2m\,E}/\hbar$. We designate the reflection coefficient by $R(k) = |r_k|^2$.

Once the reflection amplitude r_k has been obtained, the mean free-flight time τ_k of an electron may easily be found. If an electron moves with a velocity v, then per unit time it covers the distance v and may encounter an impurity with the probability $n_{\text{imp}}v$. Multiplying

0305-4470/96/227259+19$19.50

the latter with the probability $|r_k|^2$ for the electron to be scattered backwards provided an impurity has been encountered, we get the probability $1/\tau_k$ for backward scattering per unit time, and the mean free path $l_k = v\tau_k$ of an electron,

$$\frac{1}{\tau_k} = n_{\mathrm{imp}} v |r_k|^2 \qquad l_k = \frac{1}{n_{\mathrm{imp}}|r_k|^2}. \tag{1.3}$$

For weak potentials $U(x)$, the formula (1.3) reduces to the corresponding Born expression [1, equation (3.1.40)].

The fact that in 1d conductors the mean free path l_k of an electron should be inversely proportional to the *exact* reflection coefficient $R(k)$, relative to the scattering of the electron at a *single* scatterer, was first pointed out by Dunlap *et al* [2] and Wu and Phillips [3]. The principal importance of this statement lies in the fact that, due to possible resonances in the scattering, the reflection coefficient $R(k)$ may vanish for some value $k = k_n$. As is known, due to elastic scattering, electron states in 1d conductors become localized with a spatial extent of the order of l_k [4, 5]. Near the resonance, the mean free path l_k may be very large, which amounts to the appearance of extended electron states in the vicinity of the point $k = k_n$. As a result, the conductivity of a 1d conductor should significantly increase when the Fermi level coincides with the position of the resonant state on the energy axis [2, 3].

This general physical idea found its first realization in the tight-binding approximation. Introducing the random dimer model, Dunlap *et al* [2] and Wu and Phillips [3] explained the absence of localization in disordered polymers. Since then, the random dimer model and its modifications have been extensively studied [6–16]. The extended states and the suppression of localization were also found in the vicinity of resonances in the continuous Kronig–Penney model with random, short-range correlated impurities [17].

Recently, there has been a growing evidence that the extended states arising in the vicinity of resonances in the random dimer model, are rather fragile. It was shown that the on-site electron–electron interaction, or randomness in the dimer structure, as well as an external electric field destroy the extended states, the latter becoming localized [18–20]. Hence the search for physical mechanisms that could account for the observed stability of extended resonant states, has become important.

The distinguishing feature of the models investigated so far is that in all of those models the defects possessed an internal structure. It was just the internal structure of a single scatterer that led to the resonance effect and the narrow band of conducting states when the scatterers were randomly placed along a linear chain in a 1d conductor [3, 17]. As long as the internal structure of a defect is due to some kind of short-range correlations, small violations in the correlation condition may destroy the phase coherence needed for resonant states to appear [18].

It is known, however, that the internal structure of a scatterer is not necessarily needed for resonances to arise. The appearance of resonances is a quite typical phenomenon in the one-dimensional quantum scattering [21]. The resonances may well occur even if a scatterer has no visible structure. Moreover, in the present paper it is shown that, in addition to simple resonances studied previously, also much stronger 'flat' resonances are possible in the one-dimensional scattering, and this even for monomer (single) impurities. A 'flat' resonance is the vanishing of an electron's reflection coefficient $R(k)$, for some value $k = k_n$ of electron wavenumber k, as the fourth power of the difference $\Delta k = k - k_n$, i.e. $R(k) \sim (\Delta k)^4$. (We refer to a conventional resonance, with $R(k)$ vanishing as the square of the difference $R(k) \sim (\Delta k)^2$, as a 'simple' resonance).

In section 2, the existence of flat resonances in 1d scattering is demonstrated by means of a high-precision numerical solution of the Schrödinger equation for a specific, short-range impurity potential. However, rather than being an exclusive feature of the latter, this property is shared by many one-dimensional potentials (see discussion in section 4). Theoretical analysis of numerical data and the explanation of flat resonances are given in section 3. The results are discussed in section 4.

2. Flat resonances in one-dimensional scattering

For further investigation, let us specify the impurity potential $U(x)$. As a representative example, we take $U(x)$ to be

$$U(x) = -\frac{|U_0|}{\cosh(x/a)}. \tag{2.4}$$

The potential (2.4) is clearly short range so it is well suited for numerical analysis. On the other hand, the potential (2.4) belongs to a wide class of potentials whose analytic structure contains an essential element which is responsible for flat resonances. Moreover, the potential (2.4) exhibits still another interesting feature, namely, the Stokes' phenomenon in the reflection. It is discussed below in section 3.

On measuring the electron's coordinate x in units of a, we rewrite equation (1.1) in an equivalent form

$$\frac{\mathrm{d}^2\psi}{\mathrm{d}x^2} + (k_0a)^2\left[\left(\frac{k}{k_0}\right)^2 + \frac{1}{\cosh x}\right]\psi(x) = 0 \tag{2.5}$$

where $k_0 = \sqrt{2m|U_0|}/\hbar$ is the characteristic wavenumber associated with the potential $U(x)$ (2.4). The solutions of (2.5) are not known. The only information on the reflection in the potential (2.4) is the one available in the Born approximation, which yields

$$r_k^{(B)} = \frac{\pi(k_0a)^2}{2ka}\frac{1}{\cosh(\pi ka)}\mathrm{e}^{-\mathrm{i}\pi/2} \qquad ((k_0a)^2 \ll \min(ka, 1)). \tag{2.6}$$

The behaviour of the reflection coefficient $R^{(B)}(k) = |r_k^{(B)}|^2$, as given by (2.6), is rather plain: for weak potentials (2.4), $R^{(B)}(k)$ monotonically decreases with increasing $k > 0$. To see what may happen for stronger scattering potentials, let us first investigate equation (2.5) numerically.

As is known, the function r_k decreases exponentially with increasing k [22]. Let us introduce a convenient generic form for the *exact* reflection amplitude r_k by writing both its exponential factor and its phase factor explicitly, that is,

$$r_k = r_0(k)\mathrm{e}^{-\pi\beta+\mathrm{i}\phi} \qquad (k \geqslant 0) \tag{2.7}$$

the corresponding form for the exact reflection coefficient $R(k)$ being

$$R(k) = R_0(k)\,\mathrm{e}^{-2\pi\beta} \qquad R_0(k) = r_0^2(k). \tag{2.8}$$

The branch $\phi = \phi(k)$ of the phase of the reflection amplitude r_k is taken to be a continuous function of the wavenumber k. To be consistent with this choice, we have to allow the real-valued pre-exponential factor $r_0(k)$ in (2.7) to assume negative values as well as positive ones. The function $\beta = \beta(k)$, which appears in the exponent on the right-hand side of (2.7), will be chosen *for all* $k \geqslant 0$ in accordance with the semiclassical theory of one-dimensional scattering [21], i.e. for the potential (2.4) (cf section 3)

$$\begin{aligned} &\beta(k) = 2ka \qquad (k \leqslant k_0) \\ &\beta(k) = 2ka\,g(\eta) \qquad (k \geqslant k_0) \end{aligned} \tag{2.9}$$

where $\eta = k_0/k$. The function $g(\eta)$ is defined below in section 3 by (3.25*a*); it is a continuous function of k for all $k \geqslant 0$. The function $\beta(k)$ (2.9) is thus continuous but not smooth at $k = k_0$. The jump discontinuity the first derivative $\mathrm{d}\beta(k)/\mathrm{d}k$ has at $k = k_0$, is due to the semiclassical nature of expressions (2.9) (as discussed below in section 3.1). The exact reflection amplitude r_k is expected to be continuous along with its first derivative for all $k > 0$.

For the potential (2.4), we have determined the exact pre-exponential factor $r_0(k)$ in the relation (2.7), as a function of k, by means of a high-precision numerical solution of the Schrödinger equation (2.5). Namely, for each value of k given in sequence (with k_0 being fixed), equation (2.5) was solved for the wavefunction $\psi(x)$ with the boundary conditions (1.2). Then, from this numerical solution, the complex value of reflection amplitude r_k was determined. Finally, on multiplying the obtained numerical value of r_k with the factor $\exp(+\pi\beta)$ calculated for the same k according to equations (2.9) and (3.25*a*), we found the corresponding value of the factor $r_0(k)$.

In order to bring our numerical analysis closer to the region covered by the existing theory [21], and thus to verify a quantitative agreement with the latter, we have taken $k_0a = 5$. The quality of the algorithm, and the precision of calculations, were chosen to be high enough to ensure the evaluation of the factor $r_0(k)$ in (2.7) with at least five reliable digits even at the far edge of the investigated range, i.e. at $ka = 10$, where the exponential factor $\exp(-\pi\beta)$ in (2.7) is of the order of 10^{-19}.

The graph of the function $R_0(k) = r_0^2(k)$ so obtained is plotted in figure 1. For $k_0a = 5$, there are three simple resonances positioned at $ka = 3.190$ (SR1), $ka = 4.434$ (SR2), and $ka = 4.935$ (SR3), respectively, correct to three decimal places. Each simple resonance is related to a simple zero of the reflection amplitude r_k. In addition to simple resonances, the graph shows the existence of a flat resonance (FR) at $ka = 6.417$ which corresponds to a double zero of the reflection amplitude r_k.

The graph in figure 1 also reveals a drastic change in the behaviour of the reflection coefficient $R(k)$ as the wavenumber k passes through the critical value $k = k_0$ which is marked in figure 1 by the vertical broken line. Theoretical analysis of these features of the reflection is given in the next section.

3. Theory

3.1. The Stokes' phenomenon in the reflection

In the semiclassical approximation, the main features of the reflection are determined by the analytic structure of the particle's classical momentum [21] (measured in units of $\hbar/a$)

$$p(z) = (k_0a)\left[\frac{1}{\eta^2} + \frac{1}{\cosh z}\right]^{1/2} \qquad (\eta = k_0/k) \tag{3.10}$$

regarded as a function of *complex* coordinate z. The branch of the function $p(z)$ is taken to be positive for z lying on the real axis, and determined by continuity elsewhere. The semiclassical approximation is valid if, first, the parameter k_0a is large

$$k_0a \gg 1 \tag{3.11}$$

and, secondly, if the classical momentum $p(x)$ of a particle is a large and slowly varying function of the particle's real coordinate x. The exact mathematical expression for the latter property is given by Olver's condition [23, 21]

$$\int_{-\infty}^{+\infty} \left| p^{-1/2}(x)\frac{\mathrm{d}^2}{\mathrm{d}x^2}p^{-1/2}(x)\right| \mathrm{d}x \ll 1. \tag{3.12}$$

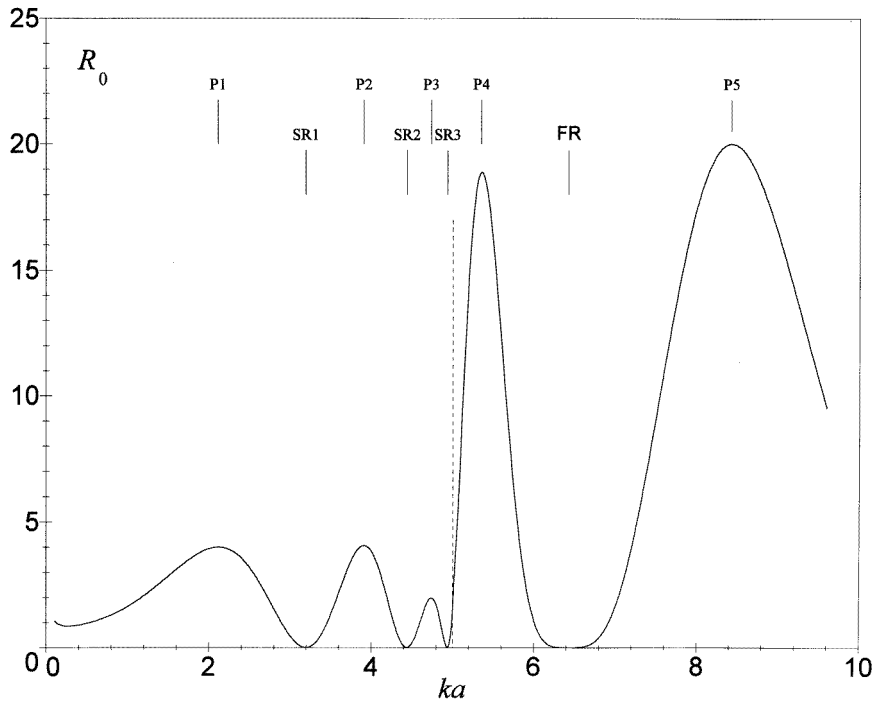

Figure 1. Pre-exponential factor $R_0(k)$ in the reflection coefficient $R(k)$ (2.8) as obtained by numerical solution of the Schrödinger equation (2.5) for the potential $U(x) = -|U_0|/\cosh(x/a)$ ($k_0a = 5$). SR1–SR3, simple resonances; FR, a 'flat' resonance; P1–P5, local maxima in the reflection. The vertical broken line marks the critical value $ka = k_0a$.

Let us investigate the analytic structure of the function $p(z)$ (3.10) relative to the potential (2.4). If the two conditions (3.11) and (3.12) are fulfilled, then only those of the singularities of $p(z)$ should be taken into account that are nearest the real axis. For all $k \geqslant 0$, there is a simple pole $s_0 = \mathrm{i}\pi/2$ of the function $U(z)$ (2.4); its position does not depend on k. As to the complex turning points (i.e. simple complex zeros of $p(z)$), their positions change with increasing k in such a way that the points move in the complex plane while tracing certain trajectories as functions of η. For the potential (2.4), two cases are to be considered. If $k \geqslant k_0$ (i.e. $\eta \leqslant 1$), then there is just one turning point z_0,

$$z_0 = \mathrm{i}\left[\frac{\pi}{2} + \arcsin(\eta^2)\right] \tag{3.13}$$

which lies in the upper half of the complex plane at a minimal distance from the real axis. As k decreases, η tends to unity from below, whereas the turning point z_0 moves along the imaginary axis towards the point $z = \mathrm{i}\pi$. The latter is attained at $k = k_0$ (i.e. $\eta = 1$).

Just at the moment, however, as k becomes smaller than k_0 ($k < k_0$, and $\eta > 1$), in place of the single turning point z_0 there appear *two* distinct turning points z_1 and z_2

$$z_1 = -\ln\left(\eta^2 + \sqrt{\eta^4 - 1}\right) + \mathrm{i}\pi \qquad z_2 = \ln\left(\eta^2 + \sqrt{\eta^4 - 1}\right) + \mathrm{i}\pi. \tag{3.14}$$

It is just the *turning point's bifurcation* that is responsible for the drastic change in the behaviour of the reflection coefficient $R(k)$, at $k = k_0$, which is displayed in figure 1. With a still further decrease in k, the two turning points z_1 and z_2 move away from the imaginary axis in opposite directions along the line $\mathrm{Im}\, z = \pi$ parallel to the real axis.

The reflection at a pair of complex-conjugate turning points (z_j, z_j^*) is described by an amplitude [21]

$$r_k(z_j) = \exp(-\pi\beta_z + \mathrm{i}\varphi_z - \mathrm{i}\pi/2) \qquad (j = 0, 1, 2) \tag{3.15}$$

where

$$\beta_z = \frac{1}{\mathrm{i}\pi}\int_{z_j^*}^{z_j} p(z)\,\mathrm{d}z \qquad \varphi_z = 2\,\mathrm{Re}\lim_{x_0\to-\infty}\left[\int_{x_0}^{z_j} p(z)\,\mathrm{d}z + kx_0\right] \qquad (\mathrm{Im}\, z_j > 0). \tag{3.16}$$

The reflection amplitude relative to a pair of complex-conjugate simple poles (s_0, s_0^*) is given by

$$r_k(s_0) = \exp(-\pi\beta_s + \mathrm{i}\varphi_s + \mathrm{i}\pi/2) \tag{3.17}$$

where

$$\beta_s = \frac{1}{\mathrm{i}\pi}\int_{s_0^*}^{s_0} p(z)\,\mathrm{d}z \qquad \varphi_s = 2\,\mathrm{Re}\lim_{x_0\to-\infty}\left[\int_{x_0}^{s_0} p(z)\,\mathrm{d}z + kx_0\right] \qquad (\mathrm{Im}\, s_0 > 0). \tag{3.18}$$

The total reflection amplitude r_k is obtained as the sum of partial reflection amplitudes $r_k(z_j)$ (3.15) and $r_k(s_0)$ (3.17), the sum extended to all reflecting points that must be taken into account.

Assuming the reflection in the potential (2.4) to be due to isolated singularities of the function $p(z)$ (3.10), we should write the total reflection amplitude r_k, for $k > k_0$, as the sum of two terms

$$r_k = r_k(z_0) + r_k(s_0) \tag{3.19a}$$

whereas for $k < k_0$ there would be the sum of three terms

$$r_k = r_k(z_1) + r_k(z_2) + r_k(s_0). \tag{3.19b}$$

Each one of the terms on the right-hand sides of equations (3.19*a*) and (3.19*b*) is an exponential of the respective type (3.15) or (3.17), with a constant coefficient that is equal to unity. The comparison of the formula (3.19*a*) with (3.19*b*) shows that, due to the turning point's bifurcation effect, there is an abrupt (dis)appearance, at $k = k_0$, of just one exponential term related to the extra turning point. Since an exponential never vanishes in the open complex plane, the total reflection amplitude r_k, as determined by the semiclassical formulae (3.19*a*) and (3.19*b*), has a jump discontinuity at $k = k_0$.

In reality, the numerical analysis shows the exact reflection coefficient $R(k)$ to be a continuous function of k (cf figure 1), as it should be [24]. The fact is that the formulae (3.19*a*) and (3.19*b*) are *asymptotic* representations of the reflection amplitude r_k under the conditions (3.11) and (3.12). For this reason, the discontinuity of the function r_k given by equations (3.19) means only that some coefficients in the *asymptotic forms* of the function r_k change abruptly as the argument k of the function passes through the critical value $k = k_0$. This event is of the same nature as the Stokes' phenomenon known in the theory of asymptotic expansions [23]. We see that the Stokes' phenomenon in one-dimensional quantum scattering appears at a critical value $k = k_c$ of the particle's wavenumber k at which the bifurcation of turning points occurs (for the specific potential (2.4), $k_c = k_0$). It manifests itself in a singular behaviour of semiclassical quantities as functions of k, at $k = k_c$. Thus, in addition to the jump discontinuities of the semiclassical expressions for r_k and $\mathrm{d}\beta(k)/\mathrm{d}k$ mentioned above, there is also a logarithmic singularity of the derivative $\mathrm{d}f(\eta)/\mathrm{d}\eta$ at $\eta = 1$, the function $f(\eta)$ being defined below by equations (3.23) and (3.42).

A more detailed investigation of coefficients in the asymptotic forms for r_k is beyond the reach of the semiclassical theory, which is asymptotic in nature. Such an investigation

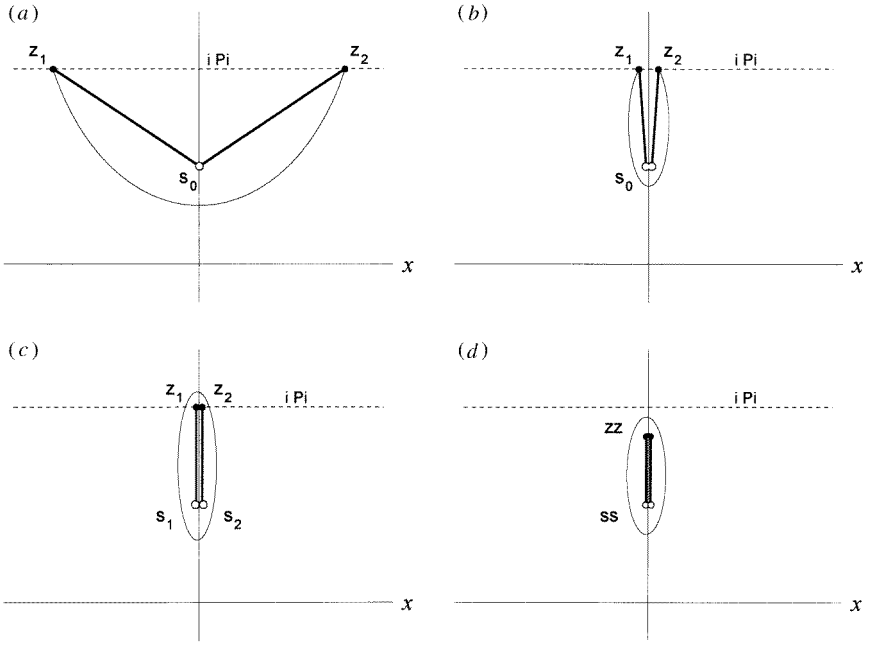

Figure 2. Typical positions of reflecting points in the upper half of the complex z-plane for the potential $U(z) = -|U_0|/\cosh z$ ($a = 1$). The positions are shown for different values of a particle's wavenumber k: (*a*) k lies to the left of the second simple resonance SR2, i.e. within the range 0–SR2 in figure 1; (*b*) the simple pole s_0 is engaged in 'doubling' when the value of k corresponds to the third local maximum P3; (*c*) $k = k_0$, the doubling of the simple pole s_0 is complete; (*d*) $k > k_0$, four coupled reflecting points zz and ss form a 'string'.

becomes possible, however, when the semiclassical expressions for r_k are considered along with numerical data on the reflection. Let us first analyse the region of lower energies $k \leqslant k_0$.

3.2. Lower energies $k \leqslant k_0$. Doubling of simple poles

For the function $p(z)$ (3.10), the integral on the left-hand side of (3.12) has the assessment

$$\int_{-\infty}^{+\infty} \left| p^{-1/2}(x) \frac{\mathrm{d}^2}{\mathrm{d}x^2} p^{-1/2}(x) \right| \mathrm{d}x \leqslant \frac{1}{2k_0 a} \left(\frac{|U_0|}{E} \right)^{1/2} \frac{|U_0|}{E + |U_0|} \tag{3.20}$$

for all $E \in (0, +\infty)$. Hence Olver's condition (3.12) yields simply $ka \gg 1$.

If k is less than k_0 but not too close to k_0, then the typical configuration of reflecting points in the upper half of the complex z-plane is shown in figure 2(*a*). The total reflection amplitude is given by the formula (3.19*b*). On substituting the expressions (3.15) and (3.17) in (3.19*b*) and then evaluating the corresponding integrals given by (3.16) and (3.18), we obtain

$$r_k = [2\cos(\pi\alpha) - \mathrm{e}^{-2\pi k a h(\eta)}]\mathrm{e}^{-\pi\beta + \mathrm{i}\varphi_{z1}} \qquad (k < k_0,\ \eta = k_0/k). \tag{3.21}$$

In (3.21), the parameter $\alpha = \alpha(k)$ is given by

$$\alpha = \frac{1}{\pi} \int_{z_1}^{z_2} p(z)\,\mathrm{d}z = 2kaf(\eta) \qquad (\eta = k_0/k) \tag{3.22}$$

where the function $f(\eta)$ is

$$f(\eta) = \frac{1}{\pi}\int_0^1 \frac{\mathrm{d}x}{\sqrt{x(1-x^2)}}\sqrt{\eta^2 - x} \qquad (\eta \geqslant 1). \tag{3.23}$$

The path of integration in (3.22) runs in the complex plane from the turning point z_1 to the turning point z_2 as shown in figure 2(a). For the parameter $\beta = \beta(k)$ in the exponent of (3.21) we obtain the expression (cf (2.9))

$$\beta = \frac{1}{\pi}\int_{z_2^*}^{z_2} p(z)\,\mathrm{d}z = 2ka[g(\eta) - h(\eta)] \qquad (\eta = k_0/k). \tag{3.24}$$

The functions $g(\eta)$ and $h(\eta)$ are found to be

$$g(\eta) = \frac{1}{\pi}\int_0^1 \frac{\mathrm{d}x}{\sqrt{x(1-x^2)}}\sqrt{x + \eta^2} \qquad (\eta \geqslant 0) \tag{3.25a}$$

$$h(\eta) = \frac{1}{\pi}\int_1^{\eta^2} \frac{\mathrm{d}x}{\sqrt{x(x^2-1)}}\sqrt{\eta^2 - x} \qquad (\eta \geqslant 1). \tag{3.25b}$$

It may be shown that, for $\eta \geqslant 1$, there is an identity

$$g(\eta) - h(\eta) = 1 \qquad (1 \leqslant \eta < \infty). \tag{3.26}$$

Substituting (3.26) in (3.24) yields $\beta = 2ka$, $(0 \leqslant k \leqslant k_0)$. The phase φ_{z1} in (3.21) is given by

$$\varphi_{z1} = -\frac{\pi}{2} + \pi\alpha + 2\,\mathrm{Re}\lim_{x_0 \to -\infty}\left[\int_{x_0}^{z_1} p(z)\,\mathrm{d}z + kx_0\right]. \tag{3.27}$$

The three functions $f(\eta)$, $g(\eta)$, and $h(\eta)$ may be expressed in terms of the hypergeometric functions of *two* variables (Appell's series $F_1(\alpha, \beta, \beta', \gamma; x, y)$ [25, vol 1, chapter 5). The graphs of the functions $f(\eta)$, $g(\eta)$, and $h(\eta)$ are plotted in figure 3. The straight chain line in figure 3 represents the common asymptote for the graphs of $f(\eta)$ and $g(\eta)$ which is described by the first term on the right-hand side of (3.29). All the three functions are seen to be continuous at the critical point $k = k_0$ (i.e. $\eta = 1$). However, the first derivatives $f'(\eta)$ and $h'(\eta)$ (with respect to η, or k) become singular at $k = k_0$. In particular, $f'(\eta)$ has a logarithmic singularity at $k = k_0$ while $h'(\eta)$ has a jump discontinuity at this point.

The function $h(\eta)$ (3.25b) vanishes at $\eta = 1$

$$h(\eta) \sim \frac{1}{\sqrt{2}}(\eta - 1) \qquad (\eta \to 1+) \tag{3.28}$$

and it monotonically increases with increasing $\eta > 1$. As $\eta \to +\infty$ (i.e. $k \to 0+$), the asymptotic form for $h(\eta)$ is

$$h(\eta) = \frac{\Gamma^2(1/4)}{(2\pi)^{3/2}}\eta - 1 + \mathrm{O}\left(\frac{1}{\eta}\right) \tag{3.29}$$

where $\Gamma(z)$ is the Gamma function.

Due to those features of the function $h(\eta)$, the second (exponential) term in the expression

$$r_0(k) = 2\cos(\pi\alpha) - \mathrm{e}^{-2\pi kah(\eta)} \tag{3.30}$$

for the pre-exponential factor $r_0(k)$ in (3.21) is negligible for all $k < k_0$ except in the vicinity of the point $k = k_0$ defined by

$$\frac{k_0 - k}{k_0} \leqslant \frac{1}{k_0 a}. \tag{3.31}$$

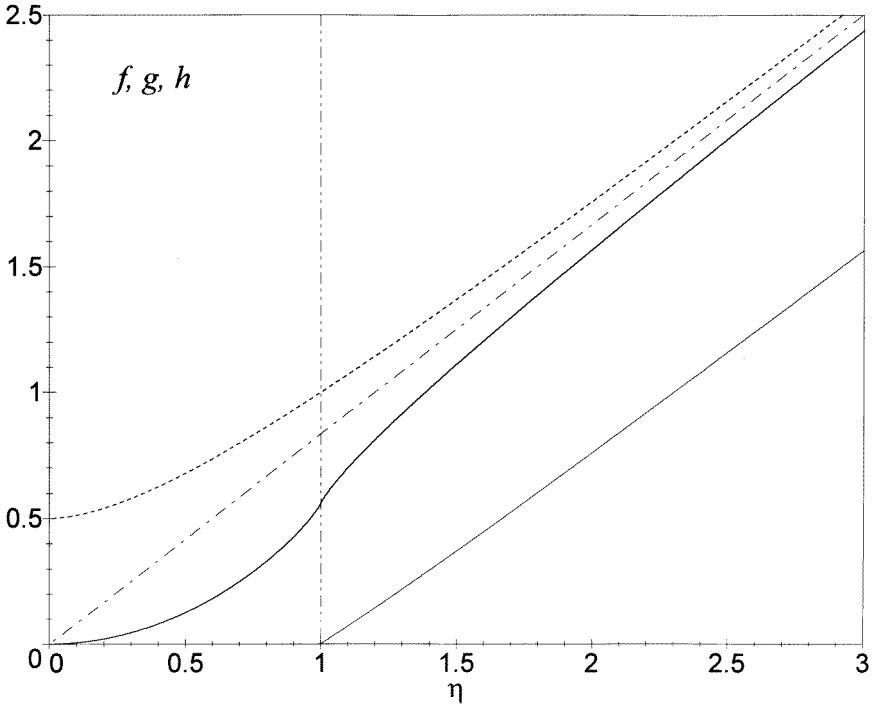

Figure 3. Graphs of the functions $f(\eta)$ (bold full curve), $g(\eta)$ (broken curve), and $h(\eta)$ (thin full curve). The chain line in the figure is described by the equation $(2\pi)^{-3/2}\Gamma^2(1/4)\eta$; it is the asymptote for the graphs of $f(\eta)$ and $g(\eta)$.

Taking into account that the exponential on the right-hand side of (3.30) comes from the simple pole s_0, we infer that, for all $k < k_0$ outside the narrow range (3.31), the reflection of a particle in the potential (2.4) is determined by the turning points z_1 and z_2 (as well as their complex conjugates). For those k, the reflection coefficient $R(k) = |r_k|^2$ is thus given by

$$R(k) = 4\cos^2(\pi\alpha)\mathrm{e}^{-4\pi ka} \qquad (ka \gg 1,\ (k_0 - k)a \geqslant 1) \tag{3.32}$$

with α defined by (3.22). Note that the exponent in (3.32) is twice as large as the one given by the Born expression (2.6) for $ka \gg 1$.

The semiclassical expression (3.30) for $r_0(k)$, with $\alpha = \alpha(k)$ given by (3.22) and (3.23), is plotted in figure 4 as the full curve that extends up to the origin $ka = 0$. The diamonds in figure 4 represent the exact values for the same function $r_0(k)$ which were obtained from the numerical solution of the Schrödinger equation as described in section 2. A good quantitative agreement is observed between the semiclassical theory (full curve in figure 4) and exact data (diamonds in figure 4), except in the neighbourhood of the point $ka = k_0a = 5$. The agreement is nearly perfect for $ka \geqslant 2$ (cf condition $ka \gg 1$ (3.20) for the semiclassical theory to be valid). The equation $\alpha = n + 1/2$ (with positive integers n) for the energies of simple resonances SR1 and SR2, which is found from the relation (3.32), coincides with the general equation (44) derived in [21]. The lowering of the local maximum P3 in the full curve, which is due to the exponential term in (3.30), is distinctly seen both in figure 4 and in figure 1.

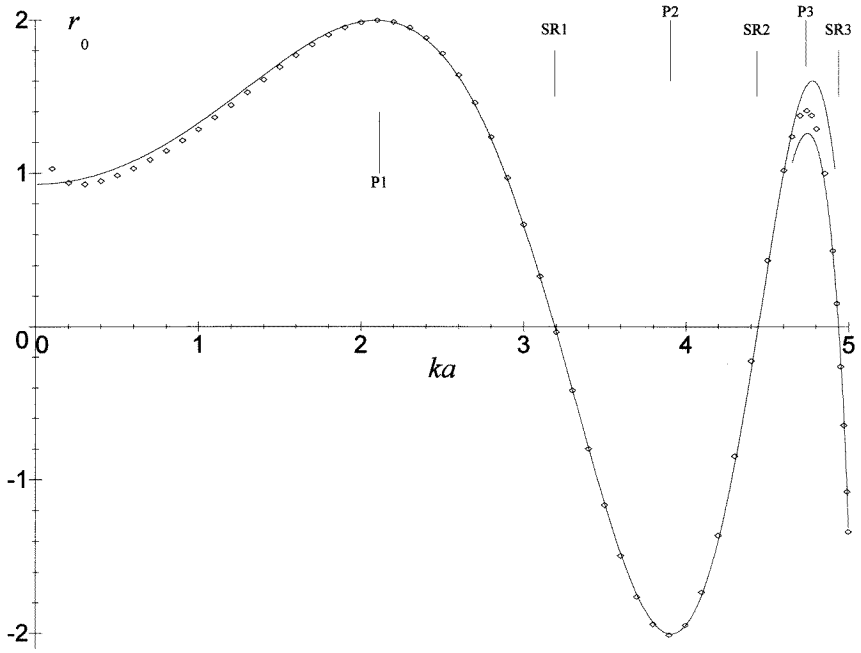

Figure 4. Pre-exponential factor $r_0(k)$ in the exact reflection amplitude r_k (2.7) for the potential $U(x) = -|U_0|/\cosh(x/a)$ ($k < k_0$, $k_0a = 5$). The diamonds represent the exact data obtained by numerical solution of the Schrödinger equation (2.5) for the potential (2.4) with $k_0a = 5$. The full curve that extends up to the origin is described by equation (3.34) with $\xi = 1$, whereas the lower curve in the neighbourhood of $ka = 5$ is described by the same equation (3.34) with $\xi = 2$.

However, as k approaches the critical value k_0, there is a growing discrepancy between the exact data, on the one hand, and the semiclassical values for $r_0(k)$ as given by the formula (3.30), on the other hand. To get an insight into what happens as $k \to k_0$, we have plotted, in the same figure 4, a fragment of another curve, the lower one, in the vicinity of the point $ka = 5$. The equation for this second (lower) full curve is

$$r_0(k) = 2\cos(\pi\alpha) - 2\mathrm{e}^{-2\pi kah(\eta)} \tag{3.33}$$

it differs from (3.30) by an additional factor 2 in front of the exponential term. We see that in a very narrow range of k in the vicinity of the critical point $k = k_0$, the diamonds in figure 4 quit the curve (3.30) and glide down to the curve (3.33). This means that, in fact, the actual values of the pre-exponential factor $r_0(k)$ are given in this range by the formula

$$r_0(k) = 2\cos(\pi\alpha) - \xi\mathrm{e}^{-2\pi ka\,h(\eta)} \tag{3.34}$$

where the coefficient $\xi = \xi(k)$ rapidly increases from $\xi = 1$ to $\xi = 2$ in a very narrow range $4.6 \leqslant ka \leqslant 4.8$ (*the Stokes' range*). It is just this rapid increase in the coefficient ξ that represents the Stokes' phenomenon in the reflection. In view of the fact that (i) the exponential term in equation (3.30), or in (3.33), is due to the simple pole s_0 of the function $U(z)$; and that (ii) the contribution of a *single* simple pole is described by the exponential (3.17) with number 1 as its coefficient, we see that the increase in the exponential's 'weight' ξ in (3.34) from 1 to 2 may be interpreted as an effective '*doubling*' of the simple pole s_0. More precisely, the *mathematical* nature of the point $z = s_0$ in the complex plane remains unalterably the same, namely, s_0 is a *simple* pole of the function $U(z)$ for all

$k \geqslant 0$. However, in the *physical* process of scattering, as the reflecting point s_0 is gradually coming on the scene with increasing k, it is progressively perceived by the quantum particle as *more than just one* reflecting point, as if being 'divided' between the two turning points z_1 and z_2. The effective configuration of reflecting points that corresponds to the local maximum P3 in figure 4, is given in figure 2(*b*). The thin curve in this figure, which joins the points z_1 and z_2 together, represents the path of integration in (3.22).

Thus, as $k \to k_0$, the numerical analysis reveals the fact that, instead of the expected disappearance of one exponential term in (3.19*b*) that is associated with one of the turning points, in reality there is the doubling of the coefficient for the exponential in (3.19*b*) that represents the simple pole. At the critical value $k = k_0$, the simple pole's doubling is complete ($\xi = 2$ in (3.34)). At the same time, the two turning points z_1 and z_2 melt into just one *geometrical* point in the complex plane while still being perceived by the particle as *two* distinct reflecting points lying on the two sides of the cut s_0–z_0. In place of two formulae (3.19*a*) and (3.19*b*), in the vicinity of the critical value $k = k_0$ there is, in fact, a single relation

$$r_k = r_k(z_1) + r_k(z_2) + r_k(s_1) + r_k(s_2) \tag{3.35}$$

that corresponds to the configuration shown in figure 2(*c*). As a result, the continuity of the reflection coefficient $R(k)$ at $k = k_0$ is ensured. From (3.35) we find the pre-exponential factor $r_0(k)$ and the reflection coefficient $R(k)$, for $k \approx k_0$,

$$r_0(k) = -4\sin^2\left(\frac{\pi\alpha}{2}\right) \qquad R(k) = 16\sin^4\left(\frac{\pi\alpha}{2}\right)\mathrm{e}^{-4\pi k_0 a} \qquad \left(0 < \frac{k_0 - k}{k_0} \ll \frac{1}{k_0 a}\right). \tag{3.36}$$

Although the formula (3.36) is valid within a narrow range of ka in the neighbourhood of $k_0 a = 5$, the change in the reflection coefficient $R(k)$ in this range, as given by (3.36), is none the less significant (cf figure 1).

3.3. Higher energies $k > k_0$. Formation of the 'string'

Further evolution of the reflecting structure in the complex plane, with increasing $k > k_0$, is shown in figure 2(*d*). There are two reflecting points zz (each one lying on the respective side of the cut s_0–z_0) with one and the same geometrical position that coincides with the position of the turning point z_0 (3.13). Also, there are two reflecting points ss (divided by the cut) with one and the same complex coordinate $z = \mathrm{i}\pi/2$, the one of the simple pole s_0. Numerical data now suggest, however, that the reflecting structure shown in figure 2(*d*) cannot be considered to be made up of four *isolated* reflecting points. Indeed, assuming the four points to be quite independent, from (3.35) we would get the following semiclassical expression for the reflection amplitude r_k

$$r_k = -4\sin^2(\pi S_k)\mathrm{e}^{-\pi\beta + \mathrm{i}\varphi_s}. \tag{3.37}$$

In (3.37), the phase φ_s is defined by

$$\varphi_s = -\frac{\pi}{2} + 2\,\mathrm{Re}\lim_{x_0 \to -\infty}\left[\int_{x_0}^{s_0} p(z)\,\mathrm{d}z + kx_0\right]. \tag{3.38}$$

For the function $\beta = \beta(k)$ in the exponent of (3.37) we find

$$\beta = \frac{1}{\pi}\int_{s_0^*}^{s_0} p(z)\,\mathrm{d}z = 2ka\,g(\eta) \qquad (\eta = k_0/k \leqslant 1) \tag{3.39}$$

with the same expression (3.25*a*) for $g(\eta)$. As η decreases from $\eta = 1$ to $\eta = 0$, the function $g(\eta)$ monotonically decreases from 1 to $\frac{1}{2}$ (cf figure 3). The function S_k in (3.37) is given by

$$S_k = \frac{1}{2\pi} \oint p(z)\,\mathrm{d}z. \tag{3.40}$$

The path of integration in (3.40) is shown in figure 2(*d*) as the closed thin curve that encircles the ensemble of reflecting points in the positive direction. On evaluating the integral in (3.40), with $p(z)$ defined by (3.10), we find

$$S_k = kaf(\eta) \qquad (\eta = k_0/k). \tag{3.41}$$

The expression for $f(\eta)$, with $\eta < 1$, is found to be (cf (3.23))

$$f(\eta) = \frac{1}{\pi} \int_0^{\eta^2} \frac{\mathrm{d}x}{\sqrt{x(1-x^2)}} \sqrt{\eta^2 - x} \qquad (\eta \leqslant 1). \tag{3.42}$$

The function $f(\eta)$ monotonically decreases with decreasing η. In particular,

$$\begin{aligned} f(\eta) &\sim \frac{2}{\pi} \ln(1+\sqrt{2}) \qquad (\eta \to 1) \\ f(\eta) &= \tfrac{1}{2}\eta^2 + \mathrm{O}(\eta^4) \qquad (\eta \to 0+). \end{aligned} \tag{3.43}$$

The pre-exponential factor $r_0(k) = -4\sin^2(\pi S_k)$, which appears on the right-hand side of (3.37), is plotted in figure 5 as the broken curve. The diamonds in this figure represent exact data obtained by a high-precision numerical solution of the Schrödinger equation (2.5). We see that the *oscillations* in the reflection amplitude r_k are in perfect agreement with the function $\sin^2(\pi S_k)$ in the formula (3.37). There are two local minima P4 and P5 at $ka = 4.736$ and $ka = 5.350$, respectively. Also, there is a 'flat' resonance FR at $ka = 6.417$, where $\sin(\pi S_k)$ vanishes. The existence of the flat resonance FR, which is thus confirmed numerically, gives evidence to the fact that, for $k > k_0$, the coefficient ξ in (3.34) is equal to 2 exactly. The general equation for the energies of flat resonances is found to be

$$S_k = \frac{1}{2\pi} \oint p(z)\,\mathrm{d}z = n \qquad (n = 1, 2, \ldots) \tag{3.44}$$

in agreement with the general equation (46*b*) [21]. At resonance values $k = k_n$ defined by (3.44), the reflection amplitude r_k vanishes as the square $(\Delta k)^2$ of the difference $\Delta k = k - k_n$. In addition, in the vicinity of a flat resonance r_k does not change its sign, unlike the behaviour of r_k in the neighbourhoods of simple resonances.

On the other hand, the *amplitude* of oscillations in r_k is found to be somewhat greater than 4, the latter being the typical value for an ensemble of four *isolated* points. In other words, the reflecting properties of the structure shown in figure 2(*d*) are close but not quite identical to those of an ensemble of four isolated reflecting points. Rather, there is a slight enhancement in the reflecting power of the four points, which may be ascribed to their mutual influence. To take the latter into account, let us introduce an additional real factor $C_s \geqslant 1$ into the formula (3.37), the latter thus becoming

$$r_k^{(S)} = -4C_s \sin^2(\pi S_k)\mathrm{e}^{-\pi\beta + \mathrm{i}\varphi_s}. \tag{3.45}$$

As is seen from figure 5, C_s is a slowly varying function of the particle's wavenumber k, considered on the scale associated with the period of oscillations in the reflection amplitude r_k (3.45). On comparing the formula (3.45) with numerical data obtained for

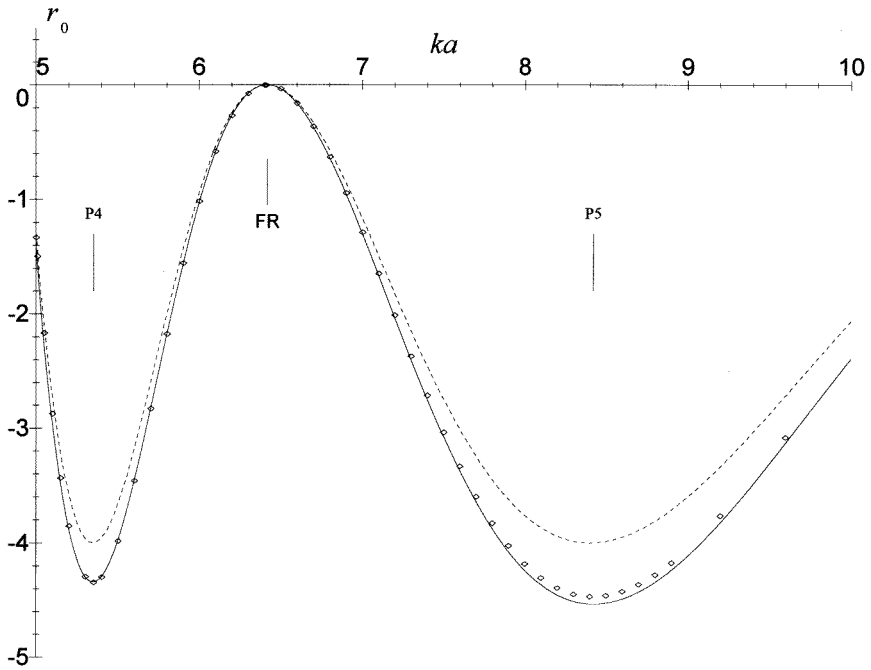

Figure 5. Pre-exponential factor $r_0(k)$ in the exact reflection amplitude r_k (2.7) for the potential $U(x) = -|U_0|/\cosh(x/a)$ ($k > k_0$, $k_0a = 5$). The full curve is described by equation (3.45) with $C_s = 1 + k/(4\pi k_0)$. The broken curve corresponds to the same equation (3.45) with $C_s = 1$. The diamonds represent the exact data as obtained from numerical solution of the Schrödinger equation (2.5) for the potential (2.4) with $k_0a = 5$.

the potentials (2.4) with various values of k_0a, we have found a uniform approximation for the correction factor C_s, as a function of k,

$$C_s = 1 + \frac{k}{4\pi k_0} \qquad (k \geqslant k_0) \tag{3.46}$$

which is valid in the investigated range $k_0a \leqslant ka < 10$. In particular, $C_s = 1.086$ at the point of the first local minimum P4, is correct to three decimal places. The slow increase in C_s is illustrated in figure 5, where the full curve represents the graph for the pre-exponential factor $r_0(k) = -4C_s \sin^2(\pi S_k)$ in (3.45) with C_s given by (3.46). Recall that the broken curve in this figure corresponds to $C_s = 1$ in equation (3.45).

Thus, as $k > k_0$, the numerical analysis displays the appearance of a new reflecting element in the analytic structure of the particle's classical momentum $p(z)$, for the potential (2.4), the element being distinct from an ensemble of isolated reflecting points. Geometrically, this element is represented (in the upper half of the complex plane) by a pair of one turning point z_0 and one simple pole s_0, which are joined together, and *split*, by a cut in the complex plane. The main distinguishing feature of such a pair is that the integral $\int_{z_0}^{s_0} p(z)\,\mathrm{d}z$, taken along the cut, turns out to be *real valued* identically with respect to the particle's energy varying in a wide range on the energy axis. We shall refer to the pair z_0–s_0 joined by a cut as the *'string'*. The physical structure of the 'string' is shown in figure 2(*d*) as an ensemble of four *coupled* reflecting points zz and ss whereas the related reflection amplitude is given by (3.45). The reflection coefficient $R_s(k)$ associated with the

'string' is readily obtained from (3.45)

$$R_s(k) = |r_k^{(S)}|^2 = 16C_s^2 \sin^4(\pi S_k)\mathrm{e}^{-2\pi\beta}. \tag{3.47}$$

It is just the formation of the 'string' in the analytic structure of the particle's classical momentum $p(z)$ that flat resonances are due to. For the potential (2.4), with $k_0a = 5$, the formula (3.47) predicts one additional flat resonance at $ka \approx 12.520$ as well as one new local maximum at $ka \approx 25.00$. As $ka > 25$, the reflection coefficient $R(k)$ monotonically falls off with increasing k while vanishing in the limit $k \to +\infty$. For $ka \gg (k_0a)^2$, the asymptotic form for $R_s(k)$ is given by

$$R_s(k) \sim C_s^2 \left[\frac{\pi(k_0a)^2}{ka}\right]^4 \mathrm{e}^{-2\pi ka} \qquad (ka \gg (k_0a)^2). \tag{3.48}$$

The exponential factor in (3.48) is just the same as given by the Born formula (2.6). However, since the asymptotic form of the correction factor C_s is not yet known for large k, there is no certainty that the pre-exponential factor in (3.48) agrees completely with that given by the Born expression (2.6). There is no general reason to believe that the latter two factors should coincide [21] because the expressions (3.48) and (2.6) are valid under different conditions.

3.4. Splitting of flat resonances in the Stokes' range

It may well happen that, for certain specific values of parameters associated with the scattering potential $U(x)$, the position of a flat resonance on the k-axis, as obtained from the semiclassical theory, falls into the Stokes' range where the coefficient $\xi = \xi(k)$ in (3.34), while rapidly increasing with k, has not yet reached its limiting value $\xi = 2$. In this narrow range, the exact reflection amplitude r_k will be asymptotically represented by equation (3.34) with a rapidly increasing function $\xi = \xi(k)$ such that $1 < \xi < 2$. As a result, instead of one double zero (flat resonance), the reflection amplitude r_k will have two closely spaced simple zeros (simple resonances) on the k-axis. This effect appears as the *splitting* of the flat resonance in the Stokes' range.

The effect of splitting of a flat resonance is illustrated in figure 6 for the potential (2.4), taken with $k_0a = 2$. For this value of k_0a, the semiclassical theory predicts only one flat resonance that falls into a close vicinity of the critical point $k = k_0$. Therefore, in place of a single flat resonance, two closely spaced simple resonances are observed in the Stokes' range, at $ka = 1.985$ and $ka = 2.229$, respectively (correct to three decimal places). For comparison, the Born approximation (2.6) for the pre-exponential factor is also represented in figure 6 (chain curve).

4. Discussion and conclusions

In problems of one-dimensional quantum scattering, the motion of a particle is not confined strictly to the real axis. Due to its ability to penetrate into classically forbidden regions, in particular, into the domains of complex coordinate z and complex momentum $p(z)$, a quantum particle moving along the real x-axis is sensitive to the singularities of the function $p(z)$ lying in the embedding complex z-plane. As a result, if there are no turning points on the real axis, the main features of the quantum scattering of a particle in a one-dimensional potential $U(x)$ are determined, in the semiclassical approximation, by the analytic structure of the particle's classical momentum $p(z)$ considered as a function of complex coordinate z. For this reason, if one and the same essential element appears in the respective analytic

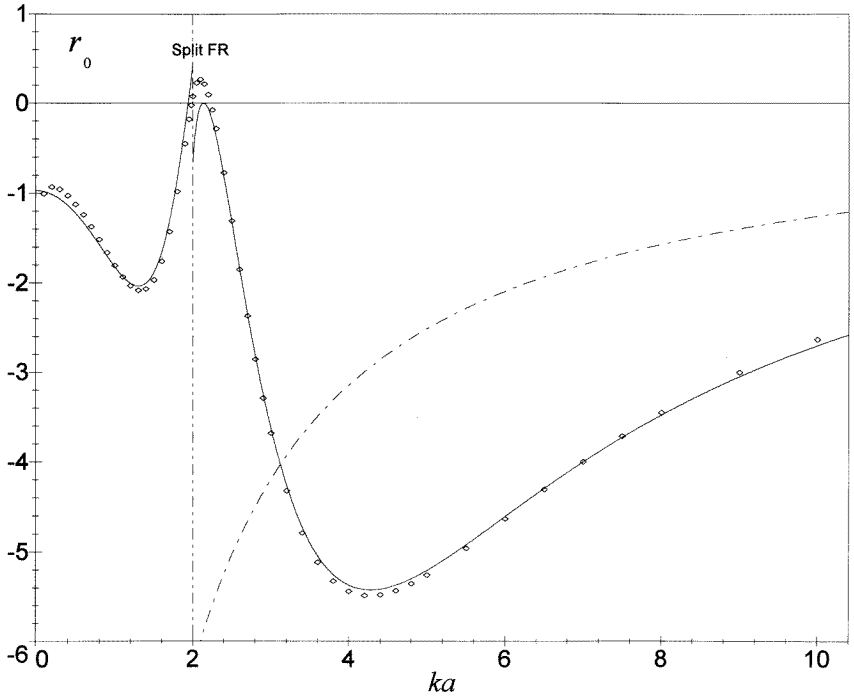

Figure 6. Splitting of a flat resonance in the Stokes' range for the potential $U(x) = -|U_0|/\cosh(x/a)$ ($k_0a = 2$). Full curves represent the semiclassical expressions for the pre-exponential factor $r_0(k)$ as given by equation (3.30) for $ka < 2$, and equation (3.45) for $ka > 2$, respectively. The correction factor C_s in equation (3.45) was chosen according to (3.46). The diamonds represent the exact data obtained from numerical solution of the Schrödinger equation (2.5) for the potential (2.4) with $k_0a = 2$. The chain curve corresponds to the Born approximation for the pre-exponential factor in (2.6).

structures associated with two different potentials, then the pictures of quantum scattering revealed by these two potentials will have similar qualitative features due to the common element. This is a kind of *similarity law* in quantum scattering.

The analytic structure of $p(z)$ is liable to appreciable changes as a function of a particle's wavenumber k. In particular, the bifurcation of turning points and the formation of a special element, called the 'string', in the analytic structure of $p(z)$, may give rise to flat resonances in the reflection. Geometrically, this element is represented (in the upper half of the complex plane) by a pair of one turning point z_0 and one simple pole s_0 (of the function $U(z)$), which are joined together, and split, by a cut in the complex plane. The main distinguishing feature of such a pair is that the integral $\int_{z_0}^{s_0} p(z)\,\mathrm{d}z$, taken along the cut, turns out to be *real valued* identically with respect to the particle's energy varying in a wide range on the energy axis. In section 3, the existence of flat resonances has been established for the *attractive* potential (2.4) ($U(x) < 0$). For attractive potentials, in the pair z_0–s_0 that forms a 'string', the simple pole s_0 lies closer to the real axis than the associated turning point z_0, i.e. $0 < \mathrm{Im}\, s_0 < \mathrm{Im}\, z_0$ (cf figure 2(*d*)). It is the presence of an *attractive* 'string' in the analytic structure of a potential that gives rise to flat resonances in quantum scattering for this potential.

The appearance of a pair of one turning point along with just one related simple pole is not at all an exclusive feature of the specific potential (2.4). This pair is frequently found with many other potentials. The simplest ones of them may be guessed while more

complicated potentials may be constructed by the methods of the theory of functions of a complex variable. The general way of constructing a scattering potential $U(x)$ with desired analytic structure consists in placing the required number of simple poles and turning points at prescribed positions in the complex plane, and then using Mittag–Leffler's theorem on meromorphic functions and Weierstrass's theorem on entire (integral) functions. To have examples different from the one investigated above (2.4), let us consider a set of potentials

$$U(x) = -|U_0| \frac{\mathrm{e}^{-\mu^2 x^2/a^2}}{1 + (x/a)^2} \tag{4.49}$$

with real constants μ. All of these potentials exhibit the bifurcation of turning points at $k = k_c$ where the critical value k_c is found to be

$$k_c = k_0 \mu \mathrm{e}^{(\mu^2+1)/2} \qquad \left(k_0 = \sqrt{2m|U_0|}/\hbar\right). \tag{4.50}$$

The evolution of the analytic structure associated with the potentials (4.49), as a function of the wavenumber k, is essentially the same as the one presented in figure 2 for the potential (2.4). Therefore the main features of quantum scattering in any one of the potentials (4.49) are determined, for $k < k_c$, by a pair of complex turning points z_1 and z_2 (cf figure 2(a)), while for $k > k_c$ there appears an attractive 'string' in the complex plane (cf figure 2(d)) that gives rise to flat resonances in the reflection. We have investigated the scattering problem for the potential (4.49), with $\mu = \frac{1}{9}$ and $k_0 a = 4$, numerically, by solving the Schrödinger equation (1.1) with boundary conditions (1.2). The exact (numerical) data so obtained have been processed in the same way as described in section 3; the data are plotted as diamonds in figure 7 which represents the pre-exponential factor $r_0(k)$ of the exact reflection amplitude r_k (2.7). For $\mu = \frac{1}{9}$, equation (4.50) yields the critical value $k_c = 0.184 k_0$ and $k_c a = 0.737$, correct to three decimal places. This value is marked in figure 7 by a vertical broken line. The full curves in this figure have been obtained from the semiclassical theory (see section 3). The correction factor C_s in equation (3.45) was taken to be

$$C_s = 1 + \frac{1}{2\pi k_0 a} \ln^2(ka + k_0 a). \tag{4.51}$$

Thus, figure 7 displays two flat resonances (FR1 and FR2), one split flat resonance (Split FR) in the Stokes' range $0.72 < ka < 0.79$, and one simple resonance (SR) in the range of lower $k < k_c$.

Figures 4–7 provide an idea on the quality of the semiclassical theory. The formal conditions for the theory to be valid, namely, (i) $k_0 a \gg 1$ (3.11) and (ii) $ka \gg 1$ (3.20), confine the applicability of the semiclassical formulae (3.32) and (3.37) to the range of k where the reflection amplitude r_k is exponentially small. However, the numerical investigation has shown the semiclassical theory to be in qualitative and fair numerical agreement with exact data even for $k_0 a \sim 1$ and $ka < 1$, i.e. in the ranges of parameters where this theory is formally not applicable. The unexpected quality of the semiclassical formulae beyond their own range of validity, is a surprising fact.

If a 'string' is found in the analytic structure of a *repulsive* potential ($U(x) > 0$), then the mutual positions of the turning point and the simple pole in the pair z_0–s_0 are interchanged, namely, it is now the turning point z_0 that is found to lie closer to the real axis than the corresponding simple pole s_0, $0 < \mathrm{Im}\, z_0 < \mathrm{Im}\, s_0$. Numerical analysis shows that, for *repulsive* 'strings', flat resonances do not appear. This problem will be the subject of a special discussion.

As far as the relation to experimental situations is concerned, the main result of this paper consists in establishing the fact that flat resonances in 1d quantum scattering *exist*. In

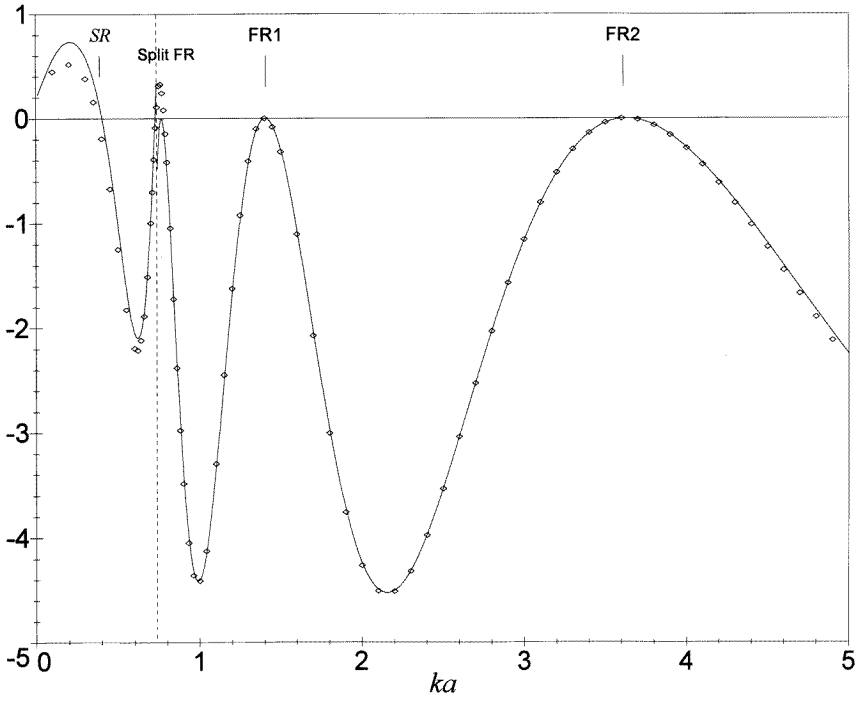

Figure 7. Pre-exponential factor $r_0(k)$ in the reflection amplitude r_k for the potential $U(x) = -|U_0|\,\mathrm{e}^{-x^2/(9a)^2}/[1 + (x/a)^2]$, $(k_0a = 4)$. The bifurcation of turning points occurs at the point $ka = k_ca = 0.737\,302$, which is marked by the vertical broken line. Full curves represent the semiclassical expressions for $r_0(k)$, as given by equation (3.30) for $ka < 2$, or by equation (3.45) for $ka > 2$, respectively. The correction factor C_s in (3.45) was taken according to equation (4.51). The diamonds represent the exact data obtained from numerical solution of the Schrödinger equation (2.5) for the potential (4.49) with $k_0a = 4$. SR, simple resonance; FR1 and FR2, 'flat' resonances. There is also one split flat resonance (Split FR) which appears as two closely spaced simple resonances in the Stokes' range at $ka = 0.733$ and $ka = 0.784$, respectively.

our opinion, it is not the question about the ways the flat resonances might come out in real crystals that should be discussed in the first place. First of all, a theoretical investigation of the localization of electron states near flat resonances is needed, including the effect of electric fields on the conductivity of electrons localized near those resonances. On comparing the theoretical predictions with experimental data, one would then see whether or not the role of flat resonances is important in the formation of electric properties of 1d disordered conductors.

The connection of the above analysis of resonances in one-dimensional quantum scattering to the theory of 1d disordered metals becomes clear in view of the discussion given in [1]. Suffice it to replace the mean free-flight time τ in [1] by the quantity τ_k (1.3), which has been investigated in the present paper. In particular, at the point of a resonance we have $1/\tau_k = 0$ so the Hamiltonian of electron-impurity interaction (the third term on the right-hand side of equation (3.2.1) in [1]) vanishes. This indicates, at least, a substantial weakening of the localization. In fact, higher-order terms in the expansion of $1/\tau_k$ in powers of the difference $k - k_n$ should be retained in order to obtain a correct Hamiltonian of electron-impurity interaction near the resonance. The results of the present paper provide

an appropriate basis for such investigation.

The number ΔN of extended states arising in the neighbourhood of a flat resonance in a 1d disordered conductor, may be estimated in the same way as used by Dunlap *et al* [2] and Phillips and Wu [3]. The linear crystal chain may be thought of as composed of N identical, equally spaced atoms with the same interatomic distance $b = N/L$. Some of the atoms are replaced at random by $N_{\rm imp}$ identical impurities so that $N_{\rm imp} \ll N$. The order of magnitude of the number ΔN of extended electron states lying in the vicinity of nth flat resonance, is determined from the relation $l_k \geqslant L$, which yields

$$\frac{\Delta N}{N} = \frac{b{\rm e}^{\pi\beta_n/2}}{2\pi\lambda_n}\left(\frac{N}{N_{\rm imp}}\right)^{1/4}\frac{1}{N^{1/4}}. \tag{4.52}$$

(The subscript n indicates that the related quantity is taken at the resonance energy $E = E_n$ which is determined from equation (3.44).) This is the number of states with average localization radius l_k being greater than the chain's length L. In (4.52), the quantity λ_n is the effective *length* associated with the string. It is equal to the derivative

$$\lambda = -\frac{\partial S_k}{\partial k} \tag{4.53}$$

of the function S_k (3.40), taken at $E = E_n$. Due to the main feature of an attractive 'string' (mentioned above in this section), λ is real valued and positive.

The relative number (4.52) of extended electron states in the neighbourhood of a flat resonance is thus proportional to $N^{-1/4}$. It is much greater than the number of extended states arising in the vicinity of a simple resonance, the latter being proportional to $N^{-1/2}$. Also, the number (4.52) is inversely proportional to the power $\frac{1}{4}$ of the dimensionless impurity concentration $N_{\rm imp}/N$. The dependence of $\Delta N/N$ on N, as given by (4.52), is quite general whereas the coefficient in (4.52) has been found in the semiclassical approximation.

Current difficulties with the theory of the random dimer model in the physics of conducting polymers, are due to the fact that extended electron states arising near resonances in this model are easily destroyed by the on-site electron–electron interactions or external electric fields (see [18–20]). This is mainly due to the fragile internal structure of random dimers which is responsible for resonances (see the discussion by Phillips and Wu [3] in the section 'Final Remarks'). Therefore, the search for physical mechanisms that could account for the observed stability of extended states in disordered polymers, has become an important problem of the condensed matter theory. In the present paper, the existence of resonances, *both simple and flat ones*, that are *not* bound to a fragile internal structure of defects, is pointed out for *single* (monomer) impurities. Therefore, the above results provide an explanation why the extended states near these resonances may survive under the effect of external perturbations.

It should be distinguished between the role of the *internal* structure of the scatterer in the formation of resonances *in general*, on the one hand, and the specific features of the scattering potential that are responsible for just *flat* resonances, on the other hand. That the internal structure of the scatterer is not at all a necessary condition for resonances to appear, *neither for simple nor for flat ones*, has been pointed out in [21] and demonstrated in the present paper (see figures 4–7). *Flat* resonances are due to a specific element (attractive 'string') which is frequently found in the analytic structures associated with quite different scattering potentials (see examples (2.4) and (4.49) investigated in this paper). For this reason, and in view of the similarity law in quantum scattering (see the first paragraph of this section), flat resonances should be regarded as a rather general phenomenon in one-dimensional scattering, not as a particular feature of very specific potentials.

In summary, flat resonances may be interesting for the physics of 1d disordered conductors for several reasons. First, the number of extended states in the neighbourhood of a flat resonance is found to be much greater than the number of extended states in the vicinity of a simple resonance. Secondly, a flat resonance differs from a simple one not only by the order of zero of the reflection coefficient $R(k)$, but also by a quite different type of phase relations for the reflected waves with closely spaced wavenumbers k in the neighbourhood of the resonance. Finally, a flat resonance is not necessarily bound to a fragile internal structure of a defect, and so it is not affected by fluctuations in correlation conditions. For all those reasons, we expect the extended states that appear in the neighbourhood of a flat resonance to stand a good chance of surviving under the effect of both electron–electron interactions and external electric fields.

References

[1] Kaner E A and Chebotarev L V 1987 *Phys. Rep.* **150** 179
[2] Dunlap D H, Wu H-L and Phillips P W 1990 *Phys. Rev. Lett.* **65** 88
[3] Phillips P and Wu H-L 1991 *Science* **252** 1805
[4] Anderson P W 1958 *Phys. Rev.* **109** 1492
[5] Mott N F and Twose W D 1961 *Adv. Phys.* **10** 107
[6] Wu H-L and Phillips P 1991 *Phys. Rev. Lett.* **66** 1366
[7] Wu H-L, Goff W and Phillips P 1992 *Phys. Rev.* B **45** 1623
[8] Evangelou S N and Katsanos D E 1992 *Phys. Lett.* **164A** 456
[9] Bovier A 1992 *J. Phys. A: Math. Gen.* **25** 1021
[10] Gangopadhyay S and Sen A K 1992 *J. Phys.: Condens. Matter* **4** 9939
[11] Datta P K, Giri D and Kundu K 1993 *Phys. Rev.* B **47** 10 727
[12] Evangelou S N and Wang A Z 1993 *Phys. Rev.* B **47** 13 126
[13] Chen X and Xiong S 1993 *J. Phys.: Condens. Matter* **5** 4029
[14] Evangelou S N, Wang A Z and Xiong S 1994 *J. Phys.: Condens. Matter* **6** 4937
[15] Lavarda F C, dos Santos M C, Galvao D S and Laks B 1994 *Phys. Rev. Lett.* **73** 1267
[16] Izrailev F M, Kottos T and Tsironis G P 1995 *Phys. Rev.* B **52** 3274
[17] Sanchez A, Macia E and Dominguez-Adame F 1994 *Phys. Rev.* B **49** 147
[18] Xiong S and Evangelou S N 1996 *Phys. Lett.* **210A** 213
[19] Da Silva C A A, de Brito P E and Nazareno H N 1995 *Phys. Rev.* B **52** 7775
[20] Ordejon P, Ortiz G and Phillips P 1994 *Phys. Rev.* B **50** 14 683
[21] Chebotarev L V 1995 *Phys. Rev.* A **52** 107
[22] Landau L D and Lifshitz E M 1977 *Quantum Mechanics* (Oxford: Pergamon)
[23] Olver F W J 1974 *Asymptotics and Special Functions* (New York: Academic)
[24] Hartman P 1964 *Ordinary Differential Equations* (New York: Wiley) ch V
[25] Bateman H and Erdélyi A 1963 *Higher Transcendental Functions* (New York: McGraw-Hill)